

The steady-state mosaic of disturbance and succession across an old-growth Central Amazon forest landscape

Jeffrey Q. Chambers^{a,b,c,1}, Robinson I. Negron-Juarez^b, Daniel Magnabosco Marra^{c,d}, Alan Di Vittorio^a, Joerg Tews^e, Dar Roberts^f, Gabriel H. P. M. Ribeiro^c, Susan E. Trumbore^d, and Niro Higuchi^c

^aClimate Sciences Department, Earth Sciences Division, Lawrence Berkeley National Laboratory, Berkeley, CA 94720; ^bEcology and Evolutionary Biology, Tulane University, New Orleans, LA 70118; ^cInstituto Nacional de Pesquisas da Amazônia, Coordenação de Pesquisas de Silvicultura Tropical, 69060-001, Manaus, Amazonas, Brazil; ^dMax Planck Institute for Biogeochemistry, 07745 Jena, Germany; ^eNoreca Consulting, Inc., Wolfville, NS, Canada B4P 2R1; and ^fGeography Department, University of California, Santa Barbara, CA 93106

Edited by Peter M. Vitousek, Stanford University, Stanford, CA, and approved December 26, 2012 (received for review February 21, 2012)

Old-growth forest ecosystems comprise a mosaic of patches in different successional stages, with the fraction of the landscape in any particular state relatively constant over large temporal and spatial scales. The size distribution and return frequency of disturbance events, and subsequent recovery processes, determine to a large extent the spatial scale over which this old-growth steady state develops. Here, we characterize this mosaic for a Central Amazon forest by integrating field plot data, remote sensing disturbance probability distribution functions, and individual-based simulation modeling. Results demonstrate that a steady state of patches of varying successional age occurs over a relatively large spatial scale, with important implications for detecting temporal trends on plots that sample a small fraction of the landscape. Long highly significant stochastic runs averaging $1.0 \text{ Mg biomass} \cdot \text{ha}^{-1} \cdot \text{y}^{-1}$ were often punctuated by episodic disturbance events, resulting in a sawtooth time series of hectare-scale tree biomass. To maximize the detection of temporal trends for this Central Amazon site (e.g., driven by CO_2 fertilization), plots larger than 10 ha would provide the greatest sensitivity. A model-based analysis of fractional mortality across all gap sizes demonstrated that 9.1–16.9% of tree mortality was missing from plot-based approaches, underscoring the need to combine plot and remote-sensing methods for estimating net landscape carbon balance. Old-growth tropical forests can exhibit complex large-scale structure driven by disturbance and recovery cycles, with ecosystem and community attributes of hectare-scale plots exhibiting continuous dynamic departures from a steady-state condition.

biodiversity | community composition | gap dynamics | NEP NEE NBP

A common assumption in old-growth forest studies is that, in the absence of a directional forcing, ecosystem characteristics and tree species composition should exhibit some type of steady-state behavior (1). Thus, plot-based studies in old-growth tropical forests that observe changing tree species composition (2), increased liana abundance (3), faster turnover rates (4), and forest biomass accumulation (5, 6), are viewed as surprising departures from an expected steady-state condition. However, disturbance events can create a landscape with patches of varying successional age, and the extent to which forest plots representatively sample this mosaic remains an open question. An important issue is how to distinguish directional trends driven by a warming climate, or rising atmospheric CO_2 concentration, from smaller-scale stochastic patterns driven by disturbance and recovery cycles (7, 8).

Over long time periods, the disturbance regime of a forested region creates a shifting steady-state mosaic, represented by patches of different successional ages, with the fraction of the landscape in any particular state remaining relatively constant over time (9, 10). In many tropical forests, gaps created by the windthrow of canopy trees is a major mode of disturbance, and specific characteristics of these gaps define key differences among regions in the development of an old-growth landscape. Following the opening of a gap, a classical ecological paradigm

describes the successional shift in community composition over time, from light-demanding pioneer and early-successional species, toward shade-tolerant late-successional and climax species (11, 12). However, most tropical forest gaps are relatively small and do not provide sufficient light to initiate secondary succession, and the related shift in community composition (13). Yet secondary succession does occur in large gaps, although these episodic succession-inducing events are rarely observed in forest plots that sample only a small portion of a landscape over a limited period (14). Because the return frequency of species-shifting gaps are not well quantified for many tropical forests, their importance in influencing biodiversity patterns (15, 16) and carbon-cycling dynamics (17, 18) remains an open question.

Gap size frequency often follows a skewed distribution (19, 20), indicating that only a portion of the disturbance spectrum is sampled over the typical spatial and temporal domains encompassed by existing forest sample plots. Thus, lacking a representative sampling of larger gaps (e.g., $>1,000 \text{ m}^2$), our understanding their effects on ecological processes is incomplete. One important observation from a tropical forest network is the increase in biomass quantified over time on fixed-area permanent sample plots, which when scaled globally accounted for $\sim 60\%$ ($1.3 \text{ Pg C} \cdot \text{y}^{-1}$) of the residual terrestrial carbon sink (6, 21). There have been broad discussions on potential causal agents driving this non-steady-state behavior, and growth fertilization of tropical trees from increasing atmospheric CO_2 has been suggested as a parsimonious explanation for some of these observations (22). However, if patches that are rapidly losing carbon following disturbance demonstrate spatial and temporal clustering, they may be underrepresented in current sampling schemes (19, 23).

To investigate the spatial scale over which an old-growth steady-state mosaic develops for a Central Amazon landscape, this study used a combination of field-based tree mortality studies, a long-term remote-sensing disturbance chronosequence (Fig. 1 and Fig. S1), and the individual-based tropical tree ecosystem and community simulator (TRECOS) model (24). To simulate the entire disturbance gradient from individual tree falls to large blowdowns, TRECOS was modified to use a gap size probability distribution function (PDF) generated from merging forest plot data and Landsat image analyses (Fig. 2 and Table 1) (*Methods*). TRECOS was then used to explore how successional patches, biomass dynamics, and large-scale carbon balance varied across a Central

Author contributions: J.Q.C., R.I.N.-J., D.M.M., S.E.T., and N.H. designed research; J.Q.C., R.I.N.-J., D.M.M., and G.H.P.M.R. performed research; J.Q.C., R.I.N.-J., A.D.V., J.T., and D.R. contributed new reagents/analytic tools; J.Q.C., R.I.N.-J., A.D.V., and J.T. analyzed data; and J.Q.C., R.I.N.-J., D.M.M., A.D.V., J.T., D.R., G.H.P.M.R., S.E.T., and N.H. wrote the paper.

The authors declare no conflict of interest.

This article is a PNAS Direct Submission.

See Commentary on page 3711.

¹To whom correspondence should be addressed. E-mail: jchambers@lbl.gov.

This article contains supporting information online at www.pnas.org/lookup/suppl/doi:10.1073/pnas.1202894110/-DCSupplemental.

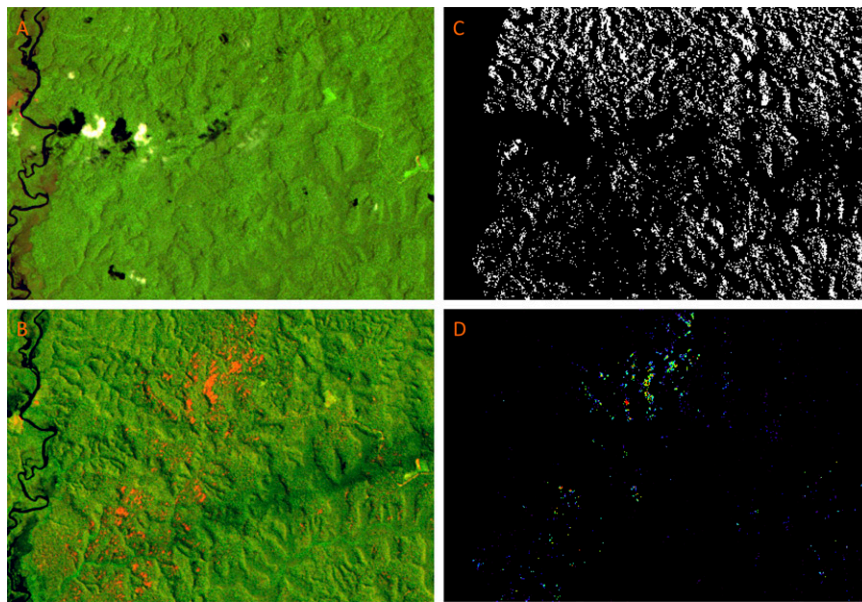


Fig. 1. A ~100-km² Central Amazon landscape shows a change in surface reflectance from (A) 2004 to (B) 2005, with patches exhibiting high short-wave infrared reflectance (red channel) indicative of disturbance across the entire image (green channel, near infrared) (B). After masking out (black pixels) all land use, rivers, roads, clouds, and areas with a high shade fraction (C), a mortality map (D) was generated based on a relationship between field-measured tree mortality and the Δ NPV remote-sensing metric. Tree mortality in this scene (D) demonstrated a variety of patch sizes ranging from isolated single-pixel disturbances, to large contiguous blowdown patches of ~30 ha.

Amazon landscape. This study provides a benchmark for exploring potential nonstochastic trends in plot-based studies, and underscores the importance of taking a landscape-scale approach in studying ecosystem processes and species distribution patterns in old-growth forest ecosystems.

Results and Discussion

A critical first step in this study was determining an average landscape-scale mortality rate for our Central Amazon site. Episodic disturbance events with return frequencies greater than

~30 y are not well represented in the existing Amazon network where plots were monitored for 4.0–21.7 y (mean of 10.9 y) up to the early 2000s (5). A plot-based study in the Central Amazon, for example, found that the largest gap occurring on 56 separate census intervals varying from 1 to 5 y on 21 single hectare permanent plots included only one eight-tree blowdown cluster, and only seven events exceeding six trees per cluster (24, 25). Thus, a plot-based mortality rate estimate for the Central Amazon of 1.02% stems-y⁻¹ (24) was entirely missing the mortality contribution of events exceeding eight trees per cluster. Fortunately, the smallest disturbance events detected in our Landsat analyses were single-pixel, approximately eight-tree fall clusters (26), and including this “episodic” Landsat-based mortality increased our regional average mortality rate for the Central Amazon from 1.02% y⁻¹ to ~1.20% y⁻¹, which was used to parameterize TRECOS (Table 1 and *SI Text*).

Multiple runs of TRECOS at 100 ha for 2,000 y were carried out to better understand the development of an old-growth Central Amazon landscape. For each run, smaller subplots were extracted from the 100-ha domain to explore how plots of varying size sampled key landscape-scale attributes. Fig. 3A derived from a typical run shows total aboveground tree biomass averaged over the entire 100-ha domain, along with five random 1-ha samples. After spinning up to steady state, the average biomass for the 100-ha plot was relatively constant, ranging from 260 to 300 Mg·ha⁻¹, which compared well with direct biomass estimates in nearby forests (27). In contrast, the single hectare plots were in constant flux, with long stretches of biomass accumulation often punctuated by episodic disturbances, and the time series rarely demonstrating steady-state behavior (Fig. 3B). The coefficient of variation (Fig. S2) for temporal change in biomass varied with plot size, with plots larger than ~10 ha providing improved sensitivity for detecting true directional trends. Based on five 1-ha samples from a typical run of TRECOS, significant linear runs in biomass gain were common, with biomass accumulation trends (mean, 0.99 Mg·ha⁻¹·y⁻¹; range, 0.75–1.49 Mg·ha⁻¹·y⁻¹) occurring twice as often as biomass loss (Fig. S3) (*SI Text*). The average accumulation rate from these purely stochastic positive

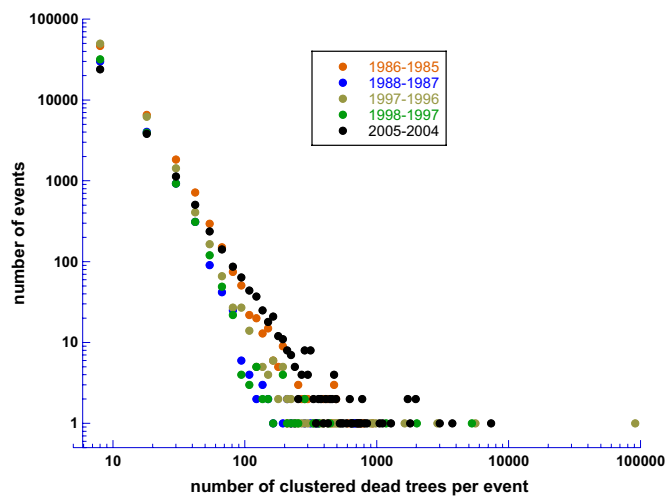


Fig. 2. A Landsat-derived frequency distribution of total number of events (y) across a range of size classes (x), with the size of the patch calculated as the total number of dead trees in the patch using the relationship between Δ NPV and the fractional mortality rate (Fig. S3). The colored symbols indicate different Landsat image pairs used to calculate Δ NPV. Summed clusters across all five Δ NPV images were used to calculate a PDF for gaps larger than approximately eight trees per gap (*SI Text*).

Table 1. The binned PDFs providing the fraction of total mortality in each event class and event probabilities (SI Text)

Minimum event PDF	Maximum event PDF	Average event PDF	Trees per event	Approximate gap area, ha	Events, ha ⁻¹ .y ⁻¹	Hectare-scale return frequency, ys	Fractional trees, ha ⁻¹ .y ⁻¹	Fractional mortality in event class, %
0.7737142	0.83992130	0.80190450	<i>1</i>		3.773830	0.26	3.774	52.0
0.1241256	0.10071330	0.11514330	<i>2</i>		0.541874	1.85	1.084	14.9
0.0735196	0.04730095	0.06238282	<i>4</i>		0.293579	3.41	1.174	16.2
0.0200586	0.00940700	0.01508790	8	0.09	0.071005	14.08	0.568	7.8
0.0057247	0.00198970	0.00384198	15	0.15	0.018081	55.31	0.271	3.7
0.0022261	0.00056755	0.00132691	33	0.30	0.006245	160.14	0.206	2.8
0.0004914	0.00008513	0.00025280	82	0.64	0.001190	840.56	0.098	1.3
0.0001090	0.00001285	0.00004844	205	1.42	0.000228	4,386.82	0.047	0.6
0.0000285	0.00000218	0.00001072	600	3.66	0.000050	19,819.34	0.030	0.4
0.0000024	0.00000010	0.00000064	2,732	14.23	0.000003	332,017.00	0.008	0.1

The average PDF was parameterized in TRECOS to distribute total landscape mortality into 10 discrete bins representing all size classes. Data for mortality events of one to four trees (in italics) are based on data from permanent forest samples plots, and the events that are not in italics or bold are from the Landsat Δ NPV analysis. The eight-tree event was estimated by merging the six- to eight-tree bin from the forest plot data (24) with the single-pixel disturbances from the Landsat analysis (26). The eight-tree bin is also the minimum size gap that initiated secondary succession, and events of this size or greater define time since episodic disturbance in TRECOS (t_e). Bold represents mortality events that are important for estimating landscape-carbon balance, yet poorly sampled with existing plots in Central Amazon forests.

runs compared well with the average biomass accumulation rate (1.22 Mg·ha⁻¹·y⁻¹) measured across a network of Amazon forest inventory plots, encompassing an average sampling period of about a decade (5).

These results demonstrate that landscape-scale estimates of Amazon forest carbon balance need to consider the full disturbance continuum (Fig. S4), from plot-based tree fall events of 1–8 trees, through intermediate-scale disturbances detectable in Landsat imagery exceeding 7–10 downed trees per cluster (26), to larger events greater than 1,000 m² (28) (Fig. S5). Although disturbance events of less than approximately five trees per gap were by far the most common (Table 1), the return frequency of episodic succession-inducing disturbance events (t_e) (i.e., greater than approximately eight trees per event) can be critical for a number of ecological and evolutionary processes. Results from TRECOS estimated the partitioning of tree mortality across all event size classes (Table 1), demonstrating that 9.1–16.9% of tree mortality was missing from plot-based approaches that poorly sample disturbance events larger than about 8–15 trees per gap. Including this episodic mortality that is generally missing from plot-based estimates would largely offset net biomass accumulation from tree recruitment and growth (27), resulting in approximate landscape carbon balance.

TRECOS predicted a median t_e at the scale of a single 400-m² grid cell of about 50 y (Fig. 4), and a hectare-scale return frequency of ~14 y (Table 1), a disturbance regime that creates the highly dynamic behavior of small forest plots in the Central Amazon (Fig. 3). This median t_e was considerably less than the time required for a forest patch to reach a mature phase (29). Thus, episodic disturbances likely play important roles in structuring tree species community composition across the landscape. Because episodic disturbances have been poorly sampled over the spatial and temporal domains encompassed by most existing Amazon forest plots, the abundance of pioneer and early successional trees species, and their roles in the community, have likely been underestimated. Likewise, tree species that are resistant to wind-throw may be relatively more abundant in areas impacted by blowdown storms. Overall, t_e is an important parameter for understanding patch-scale shifts in tree species community composition and regional biodiversity patterns (15), and tests of central biodiversity hypotheses such as niche versus neutral community assembly (14, 30), and the intermediate disturbance hypothesis (31, 32), will benefit from such a landscape-scale approach.

Tree fall gaps are also important in the cycling of carbon. Episodic disturbances create patches with a large amount of coarse woody debris (CWD), and the time required for the

decomposer community to consume this CWD and release CO₂ is much faster in Amazon forests than biomass recovery following disturbance (24). Thus, recent tree fall gaps in the early stages of succession will act as large carbon sources, followed by decades of slow carbon accumulation as trees fill the gap and species community composition changes over time. Depending on return frequencies for episodic disturbances, a balance of source and sink patches defining a steady state for atmospheric CO₂ could develop over spatial and temporal scales considerably larger than a typical forest sample plot. Because episodic disturbances occur at a frequency less than that required to attain a mature late-successional state, hectare-scale patches in the Central Amazon rarely attain maximum biomass density, creating a sawtooth pattern of biomass gain punctuated by occasional losses from succession-inducing disturbances (Fig. 3B).

Observed Amazon tree mortality and recruitment rates have increased since the mid 1970s (4), and particularly high mortality rates occurred in 2005 from drought and strong wind storms (33, 34), with the potential for additional mortality from the 2010 drought (35, 36). These high mortality events may indicate a shift toward more dynamic disturbance regimes, yet it is unknown whether this is part of a long-term climate-related trend, or a transient phenomenon. A robust prediction of many climate system models is an increase in storm strength and frequency, and a decrease in precipitation across large portions of the Southern Amazon with a warming climate (37). Because tropical precipitation in these models is generated by convective parameterizations that are highly uncertain, predicted precipitation fluxes vary widely in the tropics with a warming climate (38). However, recent work with a cloud-resolving model where no convective parameterization is needed predicts increasing tropical precipitation and storm intensity with a warming climate (39). Although it may be too early to detect directional trends in forest disturbance regimes with a changing climate, remote-sensing time series can be closely monitored for an increase in Amazon storm intensity and related disturbance regimes.

Another factor to consider is the potential for tree mortality events to drive large-scale disturbance and recovery patterns, with variation in tree mortality occurring at a variety of spatial and temporal scales in the Amazon Basin. At the landscape scale in the Central Amazon, a given mortality rate in a particular year (say 1%) is distributed among patches of varying size following a power law (Fig. S4). However, there is also temporal variability across this landscape, with year-to-year rates bounded by some minimum, and up to a maximum mortality rate averaged across a landscape of tens to hundreds of square kilometers (SI Text).

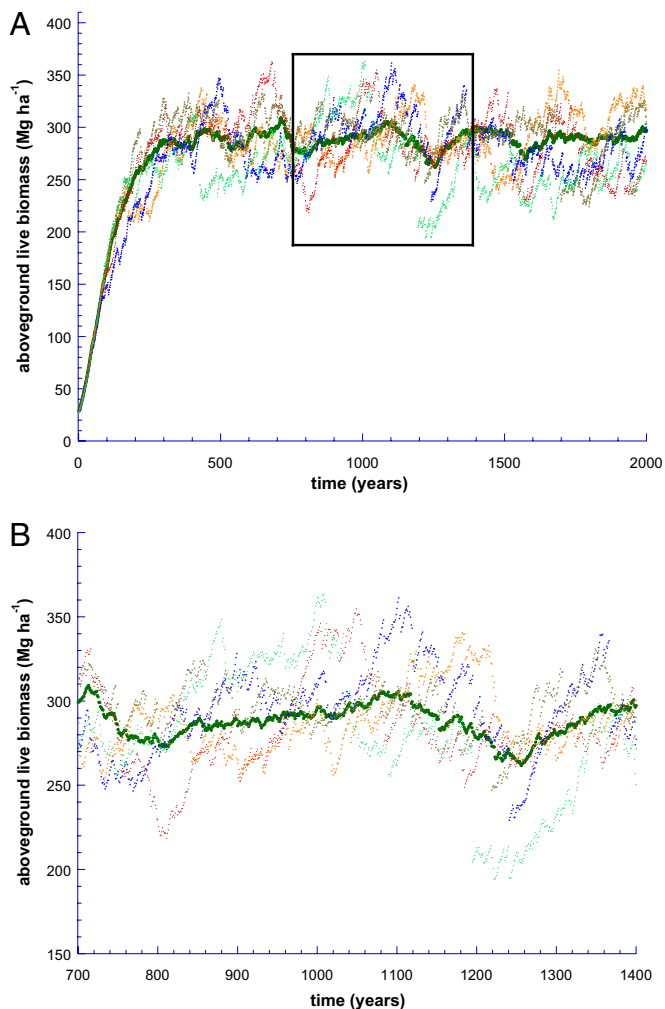


Fig. 3. (A) The 100-ha output from a single 2,000-y run of TRECOS showing temporal changes in aboveground biomass averaged over 100 ha (large dark green symbols) compared with five randomly selected 1-ha plots from within the 100-ha domain. (B) In contrast to relatively stable average tree biomass at the 100-ha scale, single hectare plots exhibited relatively continuous departures from steady state. Hectare-scale plots often demonstrated long stochastic runs of biomass accumulation punctuated by episodic biomass loss events. Trend analysis of five single hectare output plots demonstrated long, highly significant trends in biomass gain averaging ~ 1.0 Mg biomass- $\text{ha}^{-1}\cdot\text{y}^{-1}$ (Fig. S3).

At the scale of the Amazon Basin, the RAINFOR network has described remarkable gradients, with higher mortality rates in the Western Amazon, and lower rates in central and eastern portions of the basin (4). However, little is known about interannual variability in mortality at landscape to regional scales. Ultimately, any climate or CO_2 fertilization signal will be convolved with these disturbance and recovery cycles at a variety of scales, and regional approaches are needed to robustly evaluate a number of potentially confounded processes.

We demonstrate here that plots of ~ 10 ha or larger (Fig. S2) will improve our ability to detect directional biomass trends in the Central Amazon related to a warming climate (e.g., drought) or CO_2 fertilization. Networks of smaller plots may be more robust in providing average continental-scale estimates of directional change in attributes such as forest biomass accumulation (5, 6), yet it remains important to determine the size distribution of gaps on these plots with respect to variation in regional disturbance regimes. A comparison of the largest gaps

representatively sampled on the network of Amazon plots, with those observed from remote sensing imagery (e.g., Landsat), would enable an evaluation of how well the Amazon disturbance PDF, and corresponding biomass fluxes from mortality, have been sampled across the basin. Additional studies are needed on tree mortality, including PDFs of gap size, agents of mortality (e.g., drought, wind), interannual variability in landscape- to regional-scale average rates, and how all of these vary among tropical forest regions.

A number of interesting disturbance gradients across the Amazon also influence biodiversity patterns. Across the basin, average mortality rates are about twice as high on the more fertile soils of the Western Amazon than the less fertile soils of the Eastern and Central Amazon (4). Remote-sensing studies demonstrated that large blowdown gaps are much more common from near Manaus westward, compared with the less dynamic Eastern Amazon (28, 40). Ter Steege et al. (16) describe how plant functional traits covary with disturbance regimes across the Amazon basin, with heavy wooded and high seed mass trees more common in the low disturbance Guiana shield, grading to trees having low wood density and light readily dispersed seeds in the more dynamic Western Amazon. The methods used here to quantify disturbance regime attributes will be useful for better understanding the role of disturbance in structuring these Amazon tree communities. Gap size in the Manaus region, for example, followed a power law distribution with a mean scaling exponent of -2.80 (Fig. S4), and patch-scale (400 m^2) succession-inducing disturbances exhibiting a return frequency of about 50 y (Fig. 4). The distribution of gap size, and the return frequency of succession-inducing disturbances, varies across the Amazon basin, and this variation likely plays important roles in determining differences in regional tree species diversity patterns (16).

Summary

Tree mortality events ranging in size from single tree falls to large hectare-scale blowdowns create a complex disturbance and recovery mosaic in Amazon forests. If the full gap size distribution is not accounted for, plot-based approaches may undersample key attributes of this mosaic. Our results indicate that biomass accumulation trends related to stochastic processes should decrease as plot size increases, because larger plots are more likely to contain representative samples of mortality losses. In support of this assertion, a study of net carbon gain from a network of larger (16–52 ha each) tropical forest plots (41) found a significantly lower net carbon accumulation rate ($0.24 \text{ Mg C}\cdot\text{ha}^{-1}\cdot\text{y}^{-1}$) than studies using smaller plots (6) ($0.49 \text{ Mg C}\cdot\text{ha}^{-1}\cdot\text{y}^{-1}$). A plot-based approach in the Central Amazon missed up to $\sim 18\%$ of total tree mortality, comprising episodic succession-inducing tree fall clusters larger than approximately eight trees per event, with a hectare-scale return frequency of ~ 14 y (Table 1). Overall results from TRECOS demonstrated that forest plots larger than 10 ha would enable improved detection of global change signals associated with rising atmospheric CO_2 , or a warming climate.

It has long been recognized that forest sample plots are embedded in landscapes with varying disturbance regimes (15). The approach presented here enables the placement of plot-scale results into the larger context of a regional disturbance regime, including the size distribution of disturbed patches, the magnitude of disturbance within these patches, and the event return frequency. We focused primarily on how disturbance and recovery cycles affect carbon balance, but they also play important roles in influencing the distribution of tree species and community composition. This study demonstrates that efforts to determine temporal trends related to global changes should be carried out using landscape-scale approaches, including characterizing the regional disturbance regime using remote-sensing chronosequences, detailed field studies to characterize mortality events and community succession patterns,

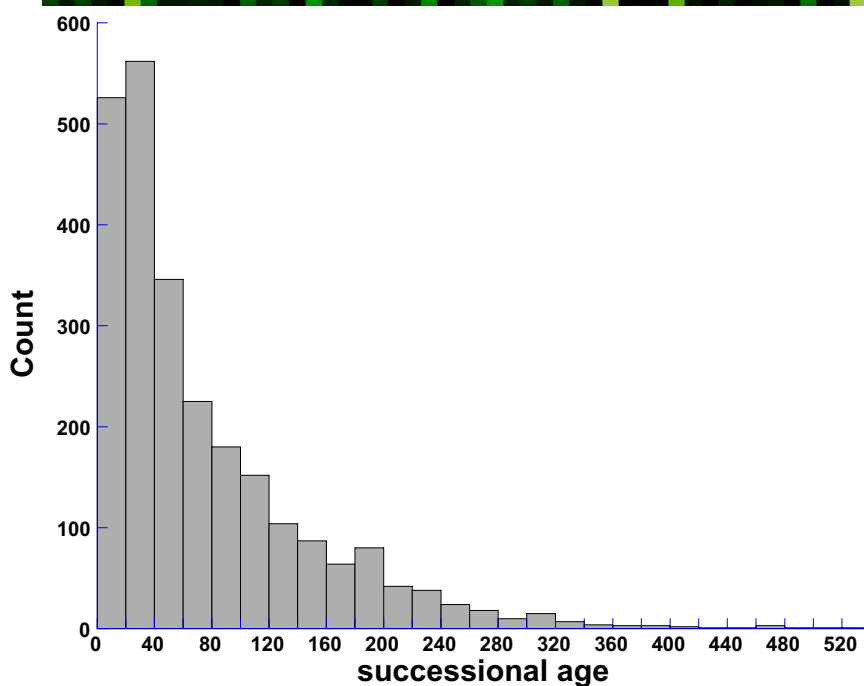
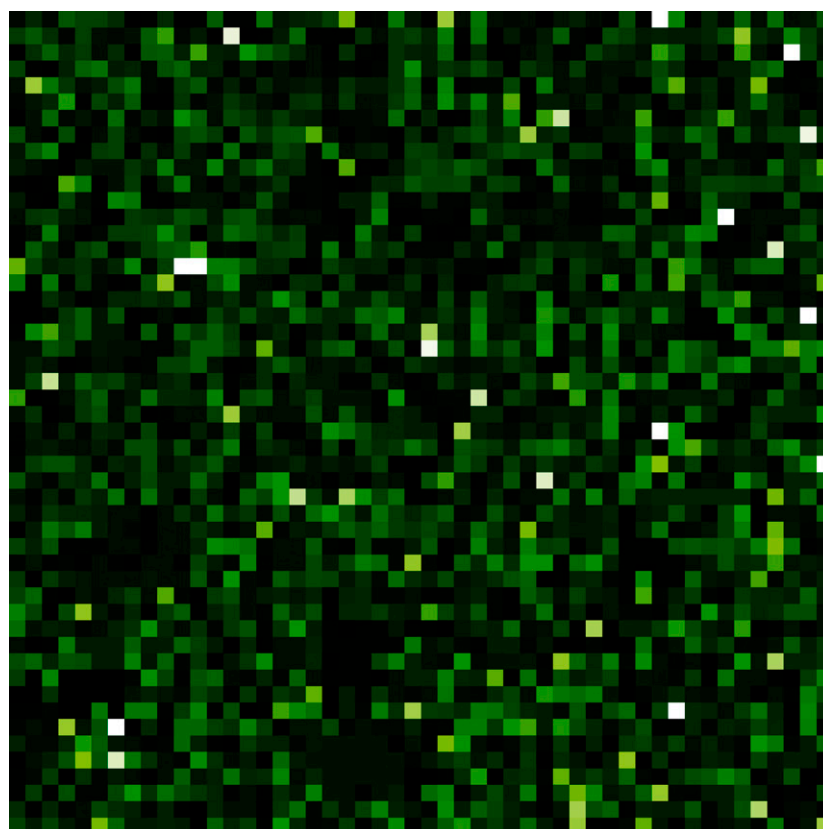


Fig. 4. Spatial distribution in time since last episodic succession-inducing disturbance (t_e) estimated from TRECOS at the end of a 2,000-y run (light pixels, old patches; dark pixels, young patches). The distribution of t_e ranging from 1 to >500 y is shown in the histogram. Median t_e for the 400-m² cells was 51 y (mean, 73.9 y), which is less than the time required for a patch to approach steady-state conditions in terms of biomass or tree species composition, resulting in a highly dynamic old-growth Central Amazon forest mosaic. Maximum t_e (534 y) demonstrated that a significant number of patches at the tail of this distribution are at a mature state, and trees exceeding 500 y are found in these forests (45).

and simulation modeling to place plot-level results into a regional context. This approach can also be used to establish important baselines for evaluating potential changes in disturbance regimes with a warming climate.

Methods

We used a total of 10 Landsat images for the Manaus region to quantify wind-driven tree mortality disturbance for five intervals (1985–1986, 1987–1988, 1996–1997, 1997–1998, 2004–2005) across an old-growth Amazon

forest landscape. Each image was processed using spectral mixture analysis whereby each pixel was unmixed into constituent spectral end-member fractions (42–44). The change in the nonphotosynthetic vegetation (wood and surface litter) fraction from one year to the next (Δ NPV) was used as the disturbance metric (33) (Fig. 1). In previous Central Amazon work, we found a strong correlation between Δ NPV and field-measured tree mortality (33) (Fig. S6), which enabled mapping mortality rates over large landscapes. In addition, we have also demonstrated the sensitivity of Landsat image analysis for detecting subpixel blowdown patches as small as 7–10 trees (26). A cluster algorithm was applied to all of the Δ NPV difference images to quantify the full size distribution of blowdown gaps up to 35 ha in patch size (>7,000 downed trees) (SI Text). The distribution of gap event size observations followed a power law distribution (Fig. 2 and Fig. S4).

Calculating a landscape-scale mortality rate presented a number of challenges. First, over the spatial and temporal domains sampled in the permanent forest plots used in this study, mortality estimates included only a single eight-tree cluster, and only seven events were recorded that exceeded six trees per cluster (24). Thus, our plot-based rates were entirely missing episodic events exceeding eight trees per cluster. To account for this mortality missing from the plot-based estimate, a landscape-scale rate was calculated that included a plot-based standing dead rate ($0.13\% \text{ y}^{-1}$), a plot-based rate for trees snapped and uprooted related to wind storms ($0.89\% \text{ y}^{-1}$) (24), and our Landsat-based wind mortality estimate ($0.18\% \text{ y}^{-1}$), giving an average landscape-scale total mortality rate of $1.20\% \text{ y}^{-1}$, which was used to parameterize TRECOS (Fig. S7). Thus, including episodic Landscape-based events increased our average regional mortality rate for the Central Amazon from $1.02\% \text{ y}^{-1}$ to $1.20\% \text{ y}^{-1}$, an 18% increase.

Most mortality events in the Central Amazon occur as lone individual trees (24), with the frequency of larger events decreasing as a potential power law function (17) (SI Text). Using data from forest inventory plots in the Central

Amazon (24) in the same region as the Landsat data, mortality events were partitioned into size classes ranging from one to eight trees per event, with a single eight-tree fall cluster the largest plot-level event observed. Scaling these probabilities over the region occupied by the Landsat Δ NPV images enabled a merging of the plot-based tree fall size class distribution and the Landsat-based distribution, with the largest plot-based event transitioning well to the smallest observed Landsat subpixel disturbances (26). The resulting PDF enabled the partitioning of a landscape-scale tree mortality rate into binned event size classes from single tree falls to large blowdowns (Table 1) (SI Text).

To better understand how intermediate-scale (episodic) disturbances influence ecosystem processes and tree species community composition, we modified an existing forest dynamics model (24). TRECOS (coded in Java) (Fig. S8) is an individual-based stochastic-empirical model that simulates all trees in 400-m^2 cells (stands) aggregated into a larger plot (e.g., 100 ha in this study), and includes information on species composition, recruitment, growth, mortality, dead tree decomposition, and other processes affecting individual trees. For this study, TRECOS was modified to use a binned PDF (Table 1) to distribute a landscape mortality rate into events of different size classes, and to simulate other key successional processes (SI Text).

ACKNOWLEDGMENTS. We thank two anonymous reviewers who provided excellent comments that led to improvements on an earlier version of this manuscript. This study was funded by the National Aeronautics and Space Administration's Biodiversity Program Project 08-BIODIV-10, Department of Energy's Office of Biological and Environmental Research Contract DE-AC02-05CH11231 under the Climate and Earth System Modeling Program, and National Aeronautics and Space Administration's Large-Scale Biosphere–Atmosphere Experiment in Amazonia–Ecology Projects CD-34 and CD-08.

- Muller-Landau HC (2009) Carbon cycle: Sink in the African jungle. *Nature* 457(7232):969–970.
- Laurance WF, et al. (2004) Pervasive alteration of tree communities in undisturbed Amazonian forests. *Nature* 428(6979):171–175.
- Phillips OL, et al. (2002) Increasing dominance of large lianas in Amazonian forests. *Nature* 418(6899):770–774.
- Phillips OL, et al. (2004) Pattern and process in Amazon tree turnover, 1976–2001. *Philos Trans R Soc Lond B Biol Sci* 359(1443):381–407.
- Baker TR, et al. (2004) Increasing biomass in Amazonian forest plots. *Philos Trans R Soc Lond B Biol Sci* 359(1443):353–365.
- Lewis SL, et al. (2009) Increasing carbon storage in intact African tropical forests. *Nature* 457(7232):1003–1006.
- Coomes DA, Holdaway RJ, Kobe RK, Lines ER, Allen RB (2012) A general integrative framework for modelling woody biomass production and carbon sequestration rates in forests. *J Ecol* 100(1):42–64.
- Körner C (2003) Atmospheric science. Slow in, rapid out—carbon flux studies and Kyoto targets. *Science* 300(5623):1242–1243.
- Bormann FH, Likens GE (1979) *Pattern and Process in a Forested Ecosystem* (Springer, New York).
- Brokaw NVL, Scheiner SM (1989) Species composition in gaps and structure of a tropical forest. *Ecology* 70(3):538–541.
- Pickett STA, White PS (1985) *The Ecology of Natural Disturbance and Patch Dynamics* (Academic, San Diego).
- Denslow JS (1987) Tropical rainforest gaps and tree species diversity. *Annu Rev Ecol Syst* 18:431–451.
- Hubbell SP, et al. (1999) Light-Gap disturbances, recruitment limitation, and tree diversity in a neotropical forest. *Science* 283(5401):554–557.
- Chambers JQ, et al. (2009) Hyperspectral remote detection of niche partitioning among canopy trees driven by blowdown gap disturbances in the Central Amazon. *Oecologia* 160(1):107–117.
- Sousa WP (1984) The role of disturbance in natural communities. *Annu Rev Ecol Syst* 15:353–391.
- ter Steege H, et al. (2006) Continental-scale patterns of canopy tree composition and function across Amazonia. *Nature* 443(7110):444–447.
- Chambers JQ, Negrón-Juárez RI, Hurr GC, Marra DM, Higuchi N (2009) Lack of intermediate-scale disturbance data prevents robust extrapolation of plot-level tree mortality rates for old-growth tropical forests. *Ecol Lett* 12:E22–E25.
- Davidson EA, et al. (2012) The Amazon basin in transition. *Nature* 481(7381):321–328.
- Fisher JL, Hurr GC, Thomas RQ, Chambers JQ (2008) Clustered disturbances lead to bias in large-scale estimates based on forest sample plots. *Ecol Lett* 11(6):554–563.
- Kellner JR, Asner GP (2009) Convergent structural responses of tropical forests to diverse disturbance regimes. *Ecol Lett* 12(9):887–897.
- Canadell JG, et al. (2007) Contributions to accelerating atmospheric CO₂ growth from economic activity, carbon intensity, and efficiency of natural sinks. *Proc Natl Acad Sci USA* 104(47):18866–18870.
- Lewis SL (2006) Tropical forests and the changing earth system. *Philos Trans R Soc Lond B Biol Sci* 361(1465):195–210.
- Körner C (2009) Responses of humid tropical trees to rising CO₂. *Annu Rev Ecol Evol Syst* 40:61–79.
- Chambers JQ, et al. (2004) Response of tree biomass and wood litter to disturbance in a Central Amazon forest. *Oecologia* 141(4):596–611.
- Chambers JQ, Higuchi N, Ferreira LV, Melack JM, Schimel JP (2000) Decomposition and carbon cycling of dead trees in tropical forests of the central Amazon. *Oecologia* 122(3):380–388.
- Negrón-Juárez RI, et al. (2011) Detection of subpixel treefall gaps with Landsat imagery in Central Amazon forests. *Remote Sens Environ* 115:3322–3328.
- Chambers JQ, Santos J, Ribeiro RJ, Higuchi N (2001) Tree damage, allometric relationships, and above-ground net primary production in a tropical forest. *For Ecol Manage* 152:73–84.
- Espirito-Santo FDB, et al. (2010) Storm intensity and old-growth forest disturbances in the Amazon region. *Geophys Res Lett* 37:L11403, 10.1029/2010GL043146.
- Saldarriaga JG, West DC, Tharp ML, Uhl C (1988) Long-term chronosequence of forest succession in the upper Rio Negro of Colombia and Venezuela. *J Ecol* 76:938–958.
- Chave J (2004) Neutral theory and community ecology. *Ecol Lett* 7(3):241–253.
- Connell JH (1978) Diversity in tropical rain forests and coral reefs. *Science* 199(4335):1302–1310.
- dos Santos FAS, Johst K, Grimm V (2011) Neutral communities may lead to decreasing diversity-disturbance relationships: Insights from a generic simulation model. *Ecol Lett* 14(7):653–660.
- Negrón-Juárez RI, et al. (2010) Widespread Amazon forest tree mortality from a single cross-basin squall line event. *Geophys Res Lett* 37:L16701.
- Phillips OL, et al. (2009) Drought sensitivity of the Amazon rainforest. *Science* 323(5919):1344–1347.
- Marengo JA, Tomasella J, Alves LM, Soares WR, Rodriguez DA (2011) The drought of 2010 in the context of historical droughts in the Amazon region. (Translated from English). *Geophys Res Lett* 38:L12703, 10.1029/2011GL047436.
- Lewis SL, Brando PM, Phillips OL, van der Heijden GMF, Nepstad D (2011) The 2010 Amazon drought. *Science* 331(6017):554–554.
- Intergovernmental Panel on Climate Change (2007) Climate change 2007: The physical science basis. In *WGI Fourth Assessment* (Intergovernmental Panel on Climate Change, Geneva), p 996.
- Kharin VV, Zwiers FW, Zhang XB, Hegerl GC (2007) Changes in temperature and precipitation extremes in the IPCC ensemble of global coupled model simulations. *J Clim* 20(8):1419–1444.
- Roms DM (2011) Response of tropical precipitation to global warming. *J Atmos Sci* 68(1):123–138.
- Nelson BW, et al. (1994) Forest disturbance by large blowdowns in the Brazilian Amazon. *Ecology* 75:853–858.
- Chave J, et al. (2008) Assessing evidence for a pervasive alteration in tropical tree communities. *PLoS Biol* 6(3):e45.
- Asner GP, et al. (2005) Selective logging in the Brazilian Amazon. *Science* 310(5747):480–482.
- Roberts DA, Smith MO, Adams JB (1993) Green-vegetation, non-photosynthetic vegetation, and soils in AVIRIS data. *Remote Sens Environ* 44:255–269.
- Souza CM, Roberts DA, Cochrane MA (2005) Combining spectral and spatial information to map canopy damage from selective logging and forest fires. *Remote Sens Environ* 98(2–3):329–343.
- Chambers JQ, Higuchi N, Schimel JP (1998) Ancient trees in Amazonia. *Nature* 391:135–136.